J. Min. Metall. Sect. B-Metall. 62 (1) (2026) 81 - 90

Journal of Mining and Metallurgy,
Section B: Metallurgy

PHASE AND ROUGHNESS ANALYSIS OF NANOCRYSTALLINE COATINGS BASED ON 310S STEEL WITH ALUMINUM ADDITIONS

Mariola Spalik [a, *], Barbara Kucharska [b], Aneta Jakubus [a], Grzegorz Krzywoszyja [a]

[a] The Jacob of Paradies University, Gorzow Wielkopolski, Poland
[b] Czestochowa University of Technology, Czestochowa, Poland

(Received 11 August 2025; Accepted 15 May 2026)

Abstract

Aluminum alloying is commonly used to improve high-temperature oxidation resistance. In this study, Al was incorporated into nanocrystalline coatings produced by magnetron sputtering of 310S chromium–nickel steel. The effect of this addition on the phase composition and morphology of the coatings, which influence the formation of protective oxide layers under high-temperature conditions, was investigated.
The coatings were analyzed using scanning electron microscopy (SEM) and atomic force microscopy (AFM), with emphasis on surface roughness, as well as X-ray diffractometry (XRD) to determine crystallite size and phase composition.
The results showed that the addition of aluminum affects phase stability in the coatings. At Al contents of 1–2 at.%, there is a twofold reduction in the fraction of the fcc phase in the coating (and its disappearance at 5 at.%), along with a similar decrease in surface roughness. At the same time, crystallite size increases while the nanocrystalline structure is retained, creating favorable conditions for the formation of dense Al_2O_3 oxide layers on the coatings.

Keywords: *Magnetron sputtering; Austenitic steel X8CrNi25-21; PVD coatings*

1. Introduction

Magnetron sputtering is a modern and widely used physical vapor deposition (PVD) technique for the production of thin coatings [1]. During the magnetron sputtering process, the coating is physically deposited from a target material that is first transformed into a plasma state (Fig. 1a) [2, 3]. This method offers extensive possibilities for the fabrication of coatings with complex chemical compositions and on substrates with diverse properties [4, 5]. The chemical composition of the coatings can be modified by incorporating alloying additions in a wide range of concentrations, regardless of their mutual solubility, unlike in conventional processing methods [6, 7]. The resulting coatings are typically characterized by a homogeneous distribution of elements throughout their volume [8, 9].

The structure and properties of PVD coatings strongly depend on the parameters of the magnetron process, as well as on the type and temperature of the substrates on which the coatings are deposited [10, 11]. Depending on these factors, the coatings may consist of micro- or nanocrystals, or even exhibit an amorphous structure, in accordance with the zone model of thin films developed by J.A. Thornton and later refined by R. Messier (Fig. 1b) [12, 13].

The nanocrystalline size of crystallites in PVD coatings has a beneficial effect on their mechanical properties (e.g., increased hardness and wear resistance), as well as on their chemical and physical properties [14–17]. According to Wagner's theory, under high-temperature oxidation conditions, nanocrystalline oxide layers form on fine-grained substrates, resulting in denser and more protective oxide scales [18]. In the case of coatings produced from sputtered stainless steels, oxidation resistance at elevated temperatures is improved, and the Cr_2O_3 oxide scale exhibits enhanced resistance to thermal shock [19]. The high-temperature oxidation resistance of steel coatings, similarly to bulk steels, can be further improved by alloying with aluminum. The primary role of Al is to promote the formation of a dense and stable Al_2O_3 oxide layer on the surface, which acts as an effective barrier against further oxidation. As a result, the incorporation of a few weight percent of aluminum can significantly enhance oxidation resistance, leading to the formation of an additional or independent Al_2O_3 scale [20–22].

Considering the nanocrystalline structure of the

Corresponding author: m.spalik@interia.pl

https://doi.org/10.2298/JMMB250811007S

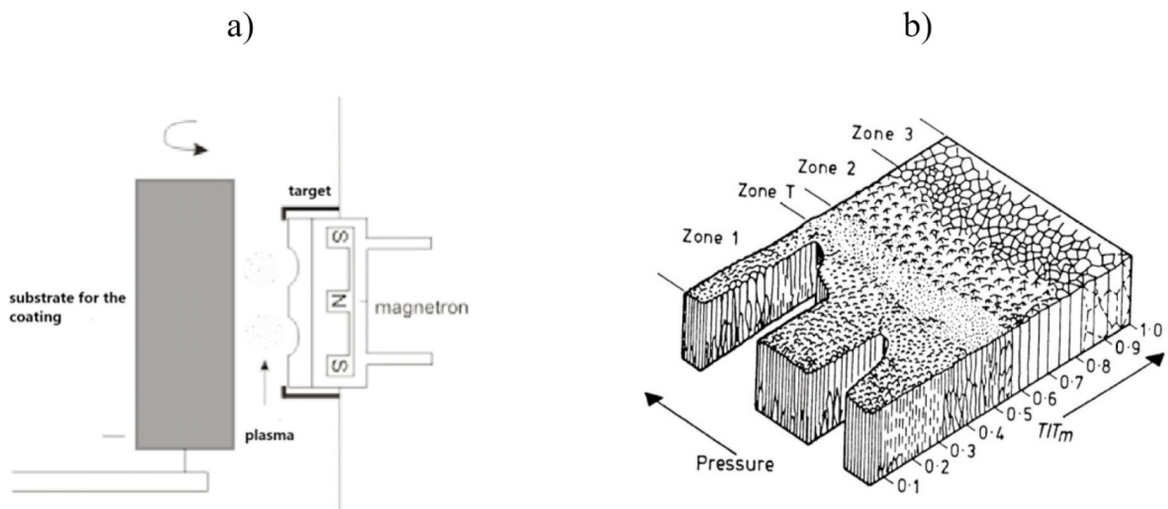

Figure 1. *Magnetron sputtering method: (a) schematic representation of the process, (b) zone (structural) model of PVD coatings (Tm – melting temperature) [12]*

coatings, the aluminum content required to form a protective and compact Al_2O_3 layer is lower than in bulk steels (typically above 5 wt.% Al) [8, 22] (Fig. 2).

Coatings produced by magnetron sputtering of austenitic steels (chromium–nickel steels of the AISI 300 series) may exhibit a nonequilibrium phase structure that differs from that of bulk austenitic steel [23, 24]. Depending on the processing conditions, the coatings may exhibit an austenitic (fcc), ferritic (bcc), or mixed ferritic–austenitic structure [8, 17, 20, 25]. Furthermore, the characteristic columnar growth associated with magnetron sputtering results in a complex and often multiphase microstructure [26].

The aim of this study was to develop chromium–nickel steel-based coatings with aluminum additions

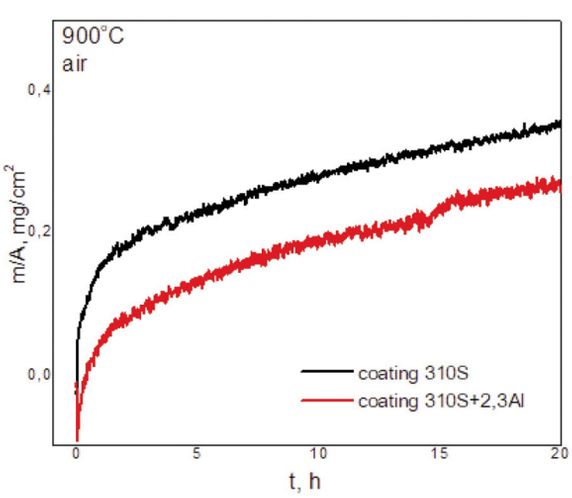

Figure 2. *Effect of Al addition on the oxidation kinetics of a 310S steel coating and a 310S steel coating containing 2.3 wt.% Al, deposited by magnetron sputtering [8]*

to enhance their high-temperature resistance and surface roughness characteristics. Such coatings are widely used in industrial applications where materials are exposed to severe thermal conditions, contributing potential applicability in systems exposed to elevated temperatures and oxidation environments. These protective systems are typically based on ceramics, high-temperature alloys, and oxide-forming coatings.

Despite the widespread application of PVD coatings based on chromium–nickel steels, the combined effect of aluminum additions on the phase composition and surface roughness of nanocrystalline coatings remains insufficiently understood. In this study, coatings were deposited on both model silicon substrates, commonly employed for precise surface and morphological characterization due to their low initial roughness, and technologically relevant steel substrates that more accurately reflect real operating conditions. The novelty of this work lies in the systematic investigation of the influence of controlled Al additions (1–5 at.%) on the structural and surface properties of magnetron-sputtered 310S-based coatings, with particular emphasis on correlating phase evolution (XRD) with nanoscale surface morphology (AFM/SEM).

The phase and roughness analysis of nanocrystalline coatings based on 310S steel with the addition of aluminum enabled the evaluation of their structure and surface properties. 310S steel, being a high-alloy austenitic stainless steel resistant to corrosion and high temperatures, may exhibit enhanced functional properties due to the application of nanocrystalline coatings. In the scientific literature, researchers investigate the effect of aluminum addition on the high-temperature resistance of Fe-Ni-

Cr-Al coatings and the mechanisms responsible for the formation of protective Al_2O_3 layers, which enhance the oxidation resistance of materials [27–29]. Particular attention is also devoted to the influence of nanocrystalline microstructure and surface condition on oxidation kinetics and the stability of protective layers [30, 31]. Liu et al. [29] investigated nanocrystalline Fe-Ni-Cr-Al coatings produced by magnetron sputtering using a composite 310S substrate, demonstrating the beneficial effect of aluminum on high-temperature oxidation resistance. Furthermore, contemporary studies focus on the relationship between nanocrystalline structure, aluminum content, and the stability of protective layers during high-temperature oxidation [33, 34]. However, only a limited number of studies concern the simultaneous analysis of phase structure and roughness parameters of nanocrystalline coatings based on 310S steel with the addition of aluminum. The novelty of the present work may be considered the detailed evaluation of the influence of aluminum addition on phase formation and surface properties of 310S coatings intended for high-temperature applications, such as gas turbine components, heat exchangers, and industrial furnace parts.

2. Materials and methods

The study material consisted of coatings deposited by magnetron sputtering of heat-resistant chromium–nickel steel AISI 310S (according to EN X8CrNi25-21), whose standard chemical composition is presented in Table 1.

Discs with a diameter of Ø100 mm were fabricated from 2 mm thick steel sheets and used as sputtering targets. The magnetron sputtering process was carried out in a B901 vacuum system (Hoch Vakuum Dresden) equipped with four magnetrons positioned at 90° relative to each other—two parallel to the chamber axis and two inclined at 60° to the chamber axis. The deposition chamber temperature ranged from 150 to 200 °C, while the substrate temperature was maintained at 150 °C. During the deposition process, the argon pressure was 0.4 Pa, the gas flow rate ranged from 23.5 to 30.6 sccm, the target-to-substrate distance was 150 mm, and the deposition rate ranged from 25 to 36 nm/min. Three targets were used during the deposition process: two steel targets and spectrally pure aluminum. The aluminum target was used to introduce Al into the steel-based coatings. The aluminum content in the coatings ranged from 1 to 5 at.%. The resulting coatings were labeled according to the aluminum content (e.g., steel+1Al).

Coatings were deposited on two types of substrates: monocrystalline Si(100) wafers and 310S steel. The silicon substrates, due to their very low initial surface roughness, were primarily used for structural and morphological characterization of the coatings, including SEM observations, XRD phase analysis, and crystallite size determination. In contrast, steel substrates were used to evaluate the surface roughness of the coatings under conditions closer to practical applications. AFM measurements were therefore performed on coatings deposited on both silicon and steel substrates, enabling a distinction between the intrinsic roughness of the coatings and the contribution of substrate-related surface features.

The study of the coatings included the determination of structural characteristics (phase composition and phase content) as well as surface morphology.

Microstructural observations were carried out using a HITACHI S-4200 scanning electron microscope (SEM). The phase structure and texture of the coatings were analyzed using X-ray diffraction (XRD) (Seifert 3003TT diffractometer, RayfleX/Analyze software) with cobalt radiation of wavelength $\lambda(K\alpha Co) = 0.17902$ nm (U = 30 kV, I = 40 mA). The diffraction patterns were recorded with a step size of 0.1–0.15° and a counting time of 4–5 s per step.

Surface morphology and roughness measurements were performed over an area of 3 × 3 μm using atomic force microscopy (AFM) in tapping mode (Veeco Multimode 5).

3. Results and discussion

Unless otherwise stated, the structural results discussed below (SEM and XRD analyses) refer to coatings deposited on monocrystalline Si substrates. AFM roughness measurements were performed for coatings deposited on both Si and steel substrates in order to distinguish intrinsic coating morphology from substrate-induced surface effects.

The coatings deposited on silicon substrates exhibited a columnar microstructure typical of PVD processes. This structural feature was reflected in the globular surface morphology observed in SEM images (Fig. 3). In comparison to coatings without aluminum, the coatings containing Al exhibited larger

Table 1. *Standard chemical composition of AISI 310S steel*

Steel	C	Cr	Ni	Si	Mn	P	S	Fe
310S	≤ 0.08	24-26	19-22	1.5	≤ 2.0	≤ 0.045	≤ 0.03	Balance

surface globules. Moreover, an increase in globule size was observed with increasing Al content, with the largest features present in the coating containing 5 at.% Al. Due to the irregular shape and multiscale nature of the surface features, although the globular morphology was not quantified using automated image analysis, SEM observations indicate an apparent increase in characteristic surface feature dimensions with increasing Al content. In particular, the coating containing 5 at.% Al exhibited visibly coarser globular features compared to the Al-free coating. Due to the irregular geometry and overlapping of the globules, these observations should be interpreted as semi-quantitative trends rather than exact measurements. Therefore, the observations presented here should be treated as indicative trends rather than precise quantitative measurements.

3.1. Phases Present in the Coatings

The diffraction patterns of the coatings are shown in Fig. 4. Despite the austenitic structure of the steel target material used for sputtering, all coatings exhibited a structure dominated by the bcc (α-Fe, ferrite) phase, which is metastable under equilibrium conditions. This phase showed a pronounced crystallographic texture, as indicated by intensity ratios deviating from standard reference patterns

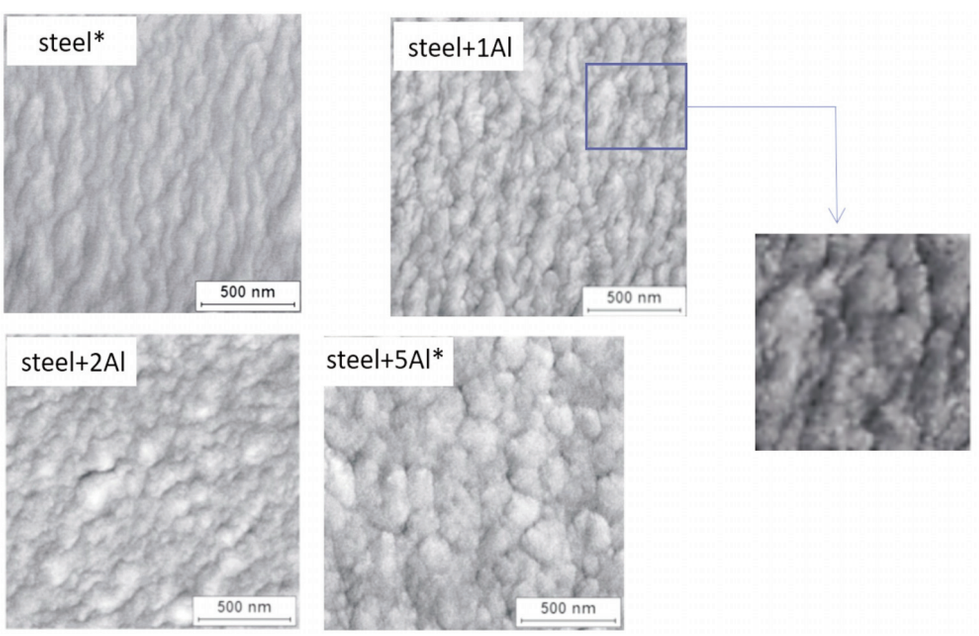

Figure 3. *Surface morphology of 310S steel coatings with different Al contents, observed by SEM (coatings deposited on silicon substrates)*

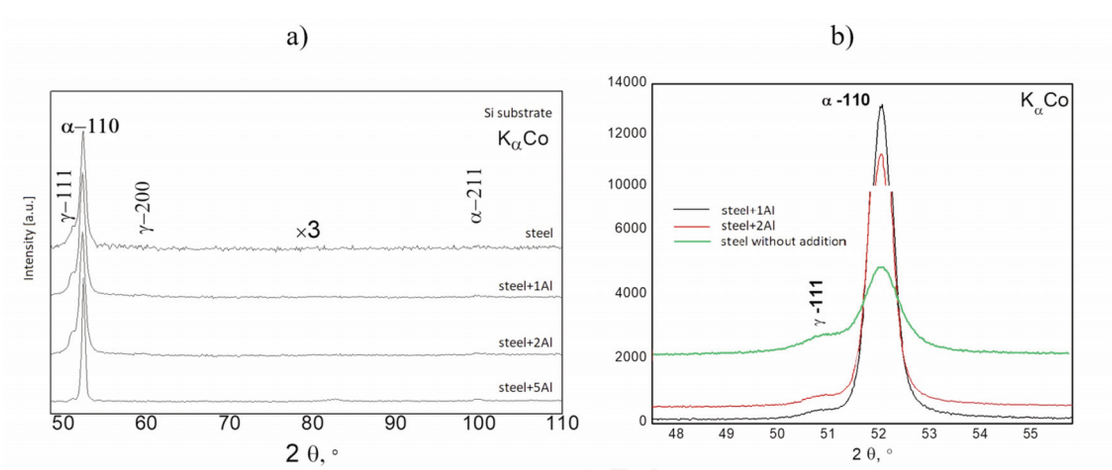

Figure 4. *X-ray diffraction patterns of 310S steel coatings with different Al contents (1–5 at.%) deposited on silicon substrates: (a) diffraction patterns of the coatings, (b) comparison of the main α-110 and γ-111 reflections*

(PDF-4+ database). In particular, an enhanced intensity of the (110) reflection and relatively lower intensities of the (211) and (200) reflections were observed (Fig. 4a).

The XRD analysis performed using Co Kα radiation revealed the presence of the fcc (γ) phase in coatings without aluminum and in coatings containing 1 and 2 at.% Al (Fig. 4b). In contrast, the fcc phase was not detected in the coating containing 5 at.% Al. Due to the applied radiation wavelength, only the main γ-111 reflection of the fcc phase was observed in the diffraction patterns (Fig. 4b). The mass absorption coefficients of the investigated coatings ranged from 142 to 151 cm²/g. This indicates that, in the angular range corresponding to the main phase reflections (2θ = 50–53°), the XRD measurements probed the entire thickness of the coatings.

Example pole figures of the α-110 planes in the coatings are presented in Figure 5. These plots illustrate the crystallographic texture of the coatings, with the intensity distributions confirming the presence of a strong preferred orientation with dominant texture component associated with the bcc phase. In the steel + 5Al coating, the texture was the strongest and can be described as fibrous, with (110) planes of the bcc phase forming preferentially parallel to the substrate surface during growth.

3.2. Phase Composition in Coatings

The presence of crystallographic texture limits the accuracy of quantitative phase analysis based on XRD measurements. However, considering that both the γ (fcc) and α (bcc) phases were formed under the same deposition conditions-i.e., under identical plasma parameters and substrate bias-it was assumed that both phases were affected by similar texture effects. Furthermore, since the phases exhibit comparable X-ray absorption coefficients, an approximate estimation of the fcc phase fraction in the coatings was performed by comparing the integrated intensities of the main reflections of both phases, namely γ-111 and α-110. The integrated intensities of these reflections were determined using pseudo-Voigt function fitting. Examples of the peak fitting procedure are shown in Fig. 6.

The fitting of the diffraction peaks using a pseudo-Voigt function was performed with Rayflex/Analyze software. An automatic selection of the Gaussian and Lorentzian components was applied. The Gaussian

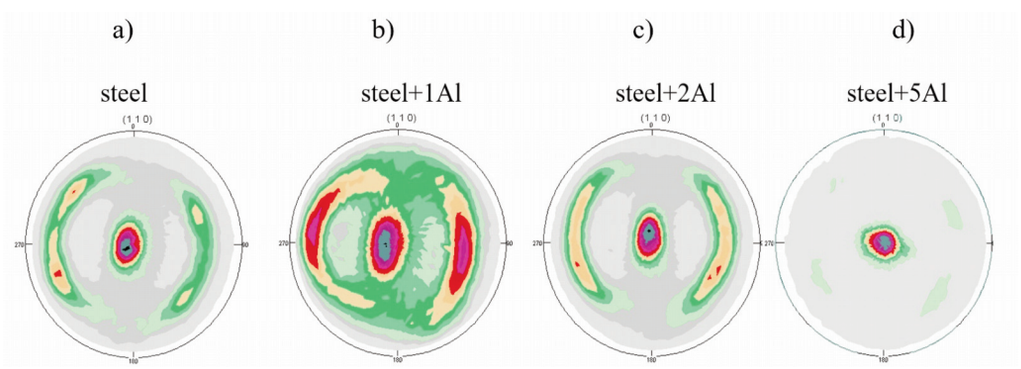

Figure 5. *Pole figures of the α-110 planes illustrating the crystallographic texture of the main phase in the coatings: (a) steel, (b) steel + 1% Al, (c) steel + 2% Al, (d) steel + 5% Al*

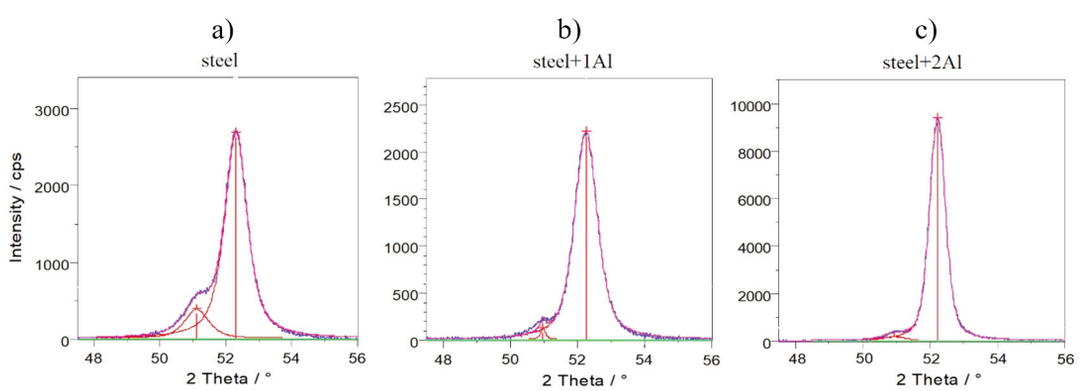

Figure 6. *Examples of pseudo-Voigt fitting of the γ-111 and α-110 reflections for 310S steel coatings: (a) steel, (b) steel + 1% Al, (c) steel + 2% Al*

fraction was approximately 0.7 for the α-110 reflection, while for the weaker γ-111 reflection it ranged from 0.7 to 1.0.

The volume fraction of the fcc phase in the coatings was estimated based on XRD measurements using Co Kα radiation and the integrated intensities of the fitted reflections. The estimated fraction of the γ phase ranged from approximately 23.5% in the coating without Al addition to about 10% in coatings containing 1–2 at.% Al. In the coating containing 5 at.% Al, the fcc phase was not detected. The results of the estimated fcc phase fractions in the coatings are presented in Fig. 7.

The crystallite sizes of the phases present in the coatings were estimated using the Scherrer method [35] based on the full width at half maximum (FWHM) of the fitted diffraction peaks. The results confirm the nanocrystalline structure of the coatings.

In the coating without Al addition, the X-ray crystallite sizes of both phases (fcc and bcc) did not exceed 12 nm. The addition of Al led to a gradual increase in the crystallite size of both phases. In the case of the bcc phase, the average crystallite size in the coating containing 5 at.% Al was approximately 20 nm (Fig. 8), as indicated by a noticeable decrease in the FWHM of the α-110 reflection.

3.3. Surface roughness of the coatings

The surface roughness of the coatings was analyzed for samples deposited on both monocrystalline silicon substrates and 310S stainless steel substrates. Although the steel substrates were mechanically polished prior to deposition, residual technological scratches remained on their surfaces. These surface features were replicated in the deposited coatings, leading to an increased overall roughness. In contrast, coatings deposited on monocrystalline silicon exhibited their intrinsic roughness, determined primarily by their microstructure and chemical composition. Therefore, the roughness of coatings deposited on steel substrates reflects a combination of the substrate roughness and the intrinsic roughness of the coatings. A comparison of surface topography for coatings deposited on silicon and steel substrates, obtained over an area of 3 × 3 μm (9 μm²), is presented in Figs. 9 and 10.

A comparison of the roughness parameters Ra, obtained from AFM areas, for coatings deposited on both substrates, measured over an area of 3x3 μm, is presented in Figure 11.

The data presented in Fig. 11 indicate that the addition of Al reduces the surface roughness of the coatings compared to the coating without additives (approximately 12 nm). The surface roughness parameter Ra of coatings containing Al ranged from 6 to 8 nm. These results suggest that the deposition of Al-containing coatings may partially reduce the contribution of substrate-related surface irregularities to the overall roughness, particularly in the case of coatings applied to real industrial substrates.

4. Summary and discussion

The results of this study indicate that coatings produced by magnetron sputtering of 310S chromium–nickel steel (X8CrNi25-21) exhibit a phase composition different from that of conventional austenitic steel in bulk form. The investigated coating, deposited on a single-crystal silicon substrate, was

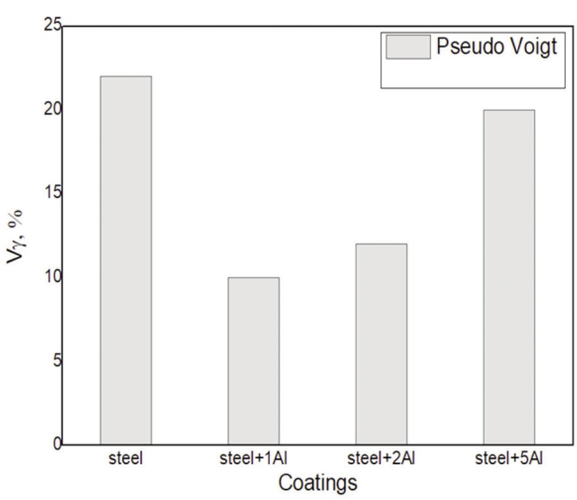

Figure 7. *Phase fractions of the fcc phase in the coatings determined from measurements using KαCo radiation based on the γ-111 and α-110 reflections described by the pseudo-Voigt functions*

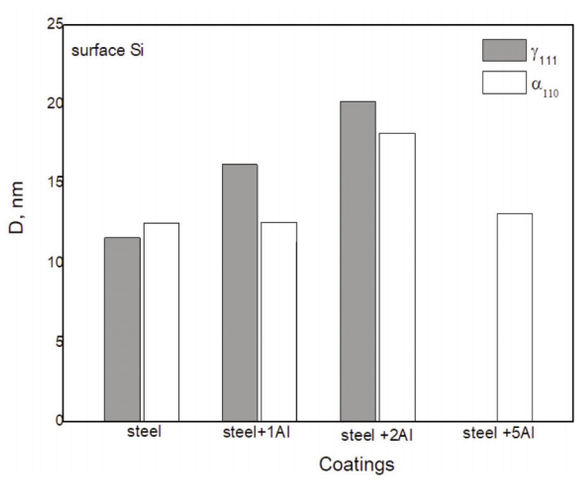

Figure 8. *X-ray crystallite size of phases in 310S steel coatings (steel, steel + 1Al, steel + 2Al, and steel + 5Al) deposited on a Si substrate*

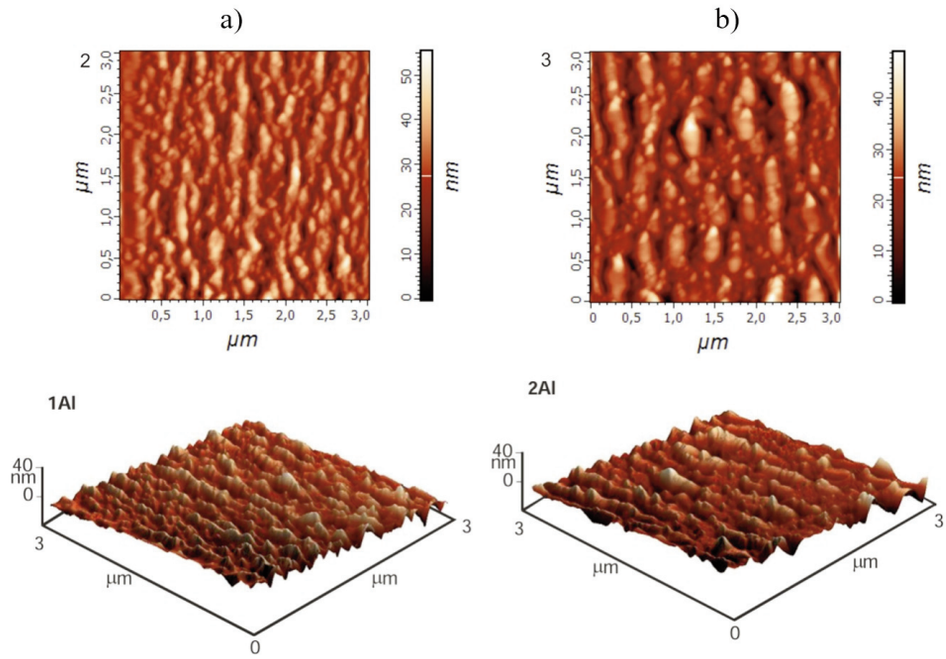

Figure 9. *2D and 3D AFM images of the surface morphology of coatings deposited on Si substrates: (a) 1% Al, (b) 2% Al*

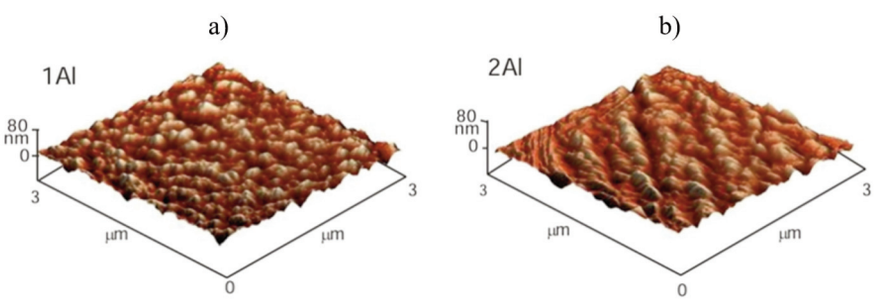

Figure 10. *2D and 3D AFM images of the surface morphology of coatings deposited on steel substrates: (a) steel + 1% Al, (b) steel + 2% Al*

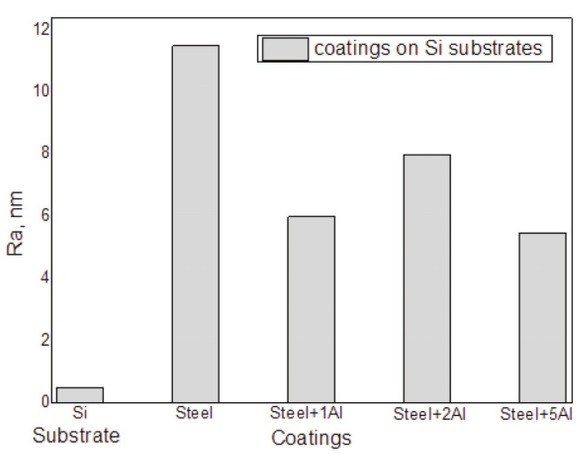

Figure 11. *Surface roughness parameter Ra for coatings deposited on steel and monocrystalline Si substrates, measured over an area of 3 × 3 µm (coating thickness: 5–6 µm)*

composed predominantly of a metastable bcc phase, while the volume fraction of the equilibrium fcc phase was approximately 23%.

The addition of 1–2 at.% Al to the coatings resulted in a further reduction of the equilibrium fcc phase fraction to approximately 10%. At an Al content of 5 at.%, the coatings exhibited a fully bcc structure. These changes in phase composition suggest a ferrite-stabilizing effect of aluminum under magnetron sputtering conditions.

The observed phase evolution may also indicate a shift of the phase boundary between the α + γ and γ regions in the Fe–Cr–Ni phase diagram due to the presence of Al in the coatings, as schematically illustrated in Fig. 12.

It should be emphasized that sputtering conditions strongly affect all coating parameters [36], and that conclusions should be drawn based on series of

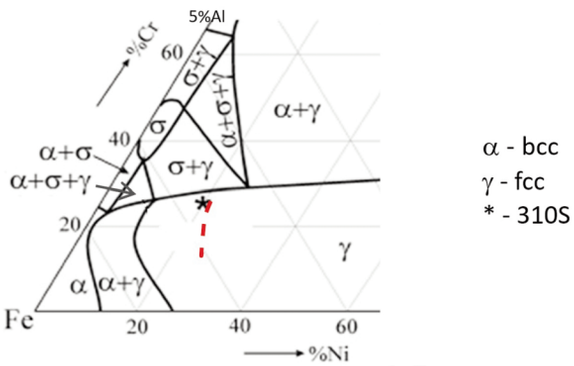

Figure 12. *Chemical composition of 310S steel (*) shown on the Fe–Cr–Ni phase diagram, with the hypothetical shift of the α+γ / γ phase boundary line resulting from magnetron sputtering and the addition of Al indicated*

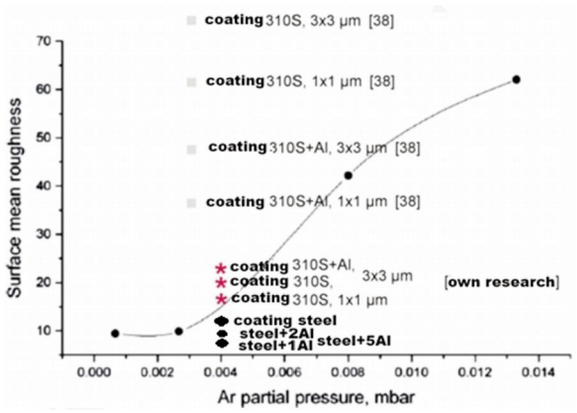

Figure 13. *Surface roughness of 310S coatings (deposited on 310S steel substrates) obtained in the present study and in the work of other authors. The figure was constructed based on Fig. 4 in the paper by Liu et al. [32]*

coatings produced under identical magnetron sputtering conditions (including, among others, the equipment, target material, and the type and positioning of substrates). For example, coatings produced by the authors using the same apparatus but in a different experimental series exhibited a fully bcc structure for a composition similar to that in the present work: 310S steel with the addition of 2.3 wt.% Al (~5 at.% Al). However, in that case, the coating of 310S steel without Al addition was also entirely bcc, unlike the coatings investigated in the present study [8].

As a result of aluminum addition, the crystallite sizes of the phases present in the coatings increased. Crystallites in the coating without Al had an average size of 12 nm, whereas in coatings containing 2–5% Al they increased to 18–20 nm. This effect of aluminum differs from the expected behavior, since a greater number of components in a magnetron-sputtered alloy usually promotes grain refinement. It can therefore be assumed that, in this case, the effect of lowering the homologous temperature (Fig. 1b) during alloy sputtering due to Al addition outweighed the influence of increased compositional complexity in the coating. Similar results were reported by other authors, including [8, 22].

The increase in crystallite size and the reduction in the fraction of the second phase resulting from the addition of 1–5% Al were accompanied by a decrease in coating roughness from approximately Ra = 12 nm to an average of about 7 nm, which important for the formation of a uniform oxide layer on the coating at elevated temperature. This observation may be beneficial from the standpoint of applying such coatings to real steel components, whose surfaces are characterized by higher roughness than the silicon substrates used in this study.

Figure 13 compares the roughness of coatings produced by the authors in the same vacuum system: the coatings investigated in the present work deposited on Si and those reported in [8] deposited on steel. For comparison, data for 310S steel coatings obtained by Liu et al. [32] and deposited on substrates of the same steel were used as a reference. Although the steel substrates used for coating deposition were polished in a similar manner, at the Ar pressure applied in the present study the Al-containing coatings deposited on Si exhibited lower roughness than the others.

5. Conclusions

The results of investigations of magnetron-deposited 310S steel coatings with 1–5 at.% Al, deposited on single-crystal Si substrates, are consistent with trends reported for sputtered Fe–Cr–Ni–Al systems, including coatings produced by other techniques such as thermal spraying. However, the strong influence of magnetron sputtering process parameters on the development of such coatings should be emphasized. Previous studies have shown that in these coatings:

- without Al addition, the structure may be two-phase (bcc/fcc) or single-phase (bcc),
- the addition of at least 5% Al leads to the disappearance of the fcc (γ) phase,
- Al addition reduces coating roughness (Ra < 8 nm) and increases the nanocrystallite size (D < 20 nm) of both bcc and fcc phases with increasing Al content in the coating.

Nanocrystalline 310S steel coatings containing up to 5 at.% Al, being single-phase and characterized by low roughness, exhibit structural features that may favor the formation of dense oxide layers during high-temperature exposure.

Control of aluminum content in the coatings can therefore be an effective tool for microstructural engineering of protective coatings, enabling the design of materials with tailored phase composition, crystallite size, and surface roughness, which may contribute to improved oxidation behavior under high-temperature conditions

Declarations

No funding was received to assist with the preparation of this manuscript.

The authors have no competing interests to declare that are relevant to the content of this article.

Data availability

The data used in this study are available from the corresponding author by request.

Author Contributions

Conceptualization: Mariola Spalik, Barbara Kucharska; Methodology: Aneta Jakubus, Mariola Spalik; Formalanalysis and investigation: Barbara Kucharska, Grzegorz Krzywoszyja; Writing - original draft preparation: Mariola Spalik, Aneta Jakubus; Writing - review and editing: Barbara Kucharska, Grzegorz Krzywoszyja; Resources: Grzegorz Krzywoszyja, Mariola Spalik; Supervision: Barbara Kucharska, Aneta Jakubus

References

[1] J. Musil, J. Vlček, A perspective of magnetron sputtering in surface engineering, Surface and Coatings Technology, 112 (1999) 162–169. https://doi.org/10.1016/S0257-8972(98)00748-8

[2] M.W. Posadowski, Nowoczesne techniki rozpylania magnetronowego, Elektronika, 4 (2006) 40–43.

[3] K. Mars, M. Sałęga-Starzecki, K.M. Zawadzka, E. Godlewska, Influence of sputtering power on the properties of magnetron sputtered tin selenide films, Materials, 17 (13) (2024) 3132. https://doi.org/10.3390/ma17133132

[4] M. Betiuk, PVD and PAPVD technologies in practice, Surface Engineering, 2 (2005) 3–13.

[5] W.M. Posadowski, A. Wiatrowski, J. Dora, Z.J. Radzimski, Magnetron sputtering process control by medium-frequency power supply parameter, Thin Solid Films, 516 (2008) 4478–4482. https://doi.org/10.1016/j.tsf.2007.05.077

[6] B. Wendler, S. Bin, Oxidation resistant FeAlCrSi and SiCx coatings on ferritic AISI 430 stainless steel, Inżynieria Materiałowa – Materials Engineering, 3–4 (2007) 804–809.

[7] Y.-C. Chang, Y.-C. Chen, C.-C. Cheng, Fabrication of AlGaN high frequency bulk acoustic resonator by reactive RF magnetron co-sputtering system, Materials, 14 (23) (2021) 7377. https://doi.org/10.3390/ma14237377

[8] B. Kucharska, PVD coatings made of chrome-nickel steel modified with Al, Ir, Re and Ru additives, Czestochowa University of Technology, Częstochowa, 2011.

[9] B. Kucharska, B. Wendler, M. Danielewski, Characteristics of AISI310S steel-based coatings deposited by magnetron sputtering on AISI 304 steel substrate, Inżynieria Materiałowa – Materials Engineering, 3 (2006) 463–466.

[10] T. Zlamal, I. Mrkvica, T. Szotkowski, S. Malotova, The influence of surface treatment of PVD coating on its quality and wear resistant, Coatings, 9 (7) (2019) 439. https://doi.org/10.3390/coatings9070439

[11] B.G. Segda, M. Jacquet, J.P. Besse, Elaboration, characterization and dielectric properties study of amorphous alumina thin films deposited by r.f. magnetron sputtering, Vacuum, 62 (2001) 27–38. https://doi.org/10.1016/S0042-207X(01)00114-2

[12] M.-J. Liu, M. Zhang, X.-F. Zhang, G.-R. Li, Q. Zhang, C.-X. Li, C.-J. Li, G.-J. Yang, Transport and deposition behaviors of vapor coating materials in plasma spray-physical vapor deposition, Applied Surface Science, 486 (2019) 80–92. https://doi.org/10.1016/j.apsusc.2019.04.224

[13] J.A. Thornton, High rate thick film growth, Annual Review of Materials Science, 7 (1977) 239–260. https://doi.org/10.1146/annurev.ms.07.080177.001323

[14] E. Locks, Q. He, J.M. De Paiva, M. Guimaraes, A.F. Arif, S.C. Veldhuis, J.R. Kish, Investigating the impact of physical vapour deposition (PVD)-coated cutting tools on stress corrosion cracking susceptibility in turning super duplex stainless steel, Coatings, 14 (3) (2024) 290. https://doi.org/10.3390/coatings14030290

[15] T. Zlamal, I. Mrkvica, T. Szotkowski, S. Malotova, The influence of surface treatment of PVD coating on its quality and wear resistant, Coatings, 9 (7) (2019) 439. https://doi.org/10.3390/coatings9070439

[16] J. Osés, G.G. Fuentes, J.F. Palacio, J. Esparza, J.A. García, R. Rodríguez, Antibacterial functionalization of PVD coatings on ceramics, Coatings, 8 (5) (2018) 197. https://doi.org/10.3390/coatings8050197

[17] B. Kucharska, Measurement of Fe-Cr-Ni coatings density in XRD analysis, Inżynieria Materiałowa – Materials Engineering, 28 (3–4) (2007) 419–421.

[18] M. Danielewski, B. Wierzba, B. Kucharska, New possibility to extend Wagner method for oxidation process modelling, Inżynieria Materiałowa – Materials Engineering, 6 (166) (2008) 830–834.

[19] W. Gao, Z. Li, Nano-structured alloy and composite coatings for high temperature application, Materials Research, 7 (1) (2004) 175–182. https://doi.org/10.1590/S1516-14392004000100023

[20] Z. Liu, W. Gao, M. Li, Cyclic oxidation of sputter-deposited nanocrystalline Fe-Cr-Ni-Al alloy coatings, Oxidation of Metals, 51 (5–6) (1999) 51–63. https://doi.org/10.1023/A%3A1018835126181

[21] B. Wendler, S. Bin, Oxidation resistant FeAlCrSi and SiCx coatings on ferritic AISI 430 stainless steel, Inżynieria Materiałowa – Materials Engineering, 3–4 (2007) 804–809.

[22] M. Mróz, S. Olszewska, P. Rąb, Evaluation of the possibility to improve the scratch resistance of the AZ91 alloy by applying a coating, Archives of Foundry

Engineering, 4 (2023) 157–162. https://doi.org/10.24425/afe.2023.146690

[23] H. Kun, H. Gong, K. Zeng, Z. Li, W. Gao, Oxidation behaviour of stainless steel-A1 coatings produced by co-sputtering and reactive sputtering, Materials Letters, 46 (2000) 53–59. https://doi.org/10.1016/S0167-577X(00)00142-7

[24] B. Kucharska, Diffractometric examination of the structure of heat-resisting steel-based coatings in different measurement geometries, Central European Journal of Physics, 9 (5) (2011) 1294–1300. https://doi.org/10.2478/s11534-011-0027-2

[25] X. Zhang, A. Misra, R.K. Schulzer, C.J. Wetteland, H. Wang, M. Nastasi, Critical factors that determined face-centered to body-centered cubic phase transformation in sputter-deposited austenitic stainless steel films, Vacuum, 66 (2002) 257–261. https://doi.org/10.1557/JMR.2004.0215

[26] P. Dasgupta, On use of pseudo-Voigt profiles in diffraction line broadening analysis, Fizika A, 9 (2) (2000) 61–66.

[27] Z. Liu, W. Gao, Y.He, Oxidation behaviour of nanocrystalline Fe–Ni–Cr–Al alloy coatings, Materials Science and Technology, 15 (12) (1999) 1447-1450. https://doi.org/ 10.1179/026708399101505446

[28] Y. Karanth, S. Sharma, K. Darling, H. El Kadiri, K. Solanki, Oxidation Behavior of Nanocrystalline Alloys, Materials. 17 (23) 5842 (2024). https://doi.org/10.3390/ma17235842

[29] N. Birbilis, J. Zhang, R Gupt, Oxidation Resistance of Nanocrystalline Alloys, in Corrosion Resistance. InTech. (2012). https://doi.org/10.5772/34928

[30] W.J. Nowak, D. Serafin, B. Wierzba, Effect of surface mechanical treatment on the oxidation behavior of FeAl-model alloy, Journal of Materials Science 54, 9185–9196 (2019). https://doi.org/10.1007/s10853-019-03509-5

[31] W.J.Nowak, B. Wierzba, Effect of Surface Treatment on High-Temperature Oxidation Behavior of IN 713C. Journal of Materials Engineering and Performance 27, 5280–5290 (2018). https://doi.org/10.1007/s11665-018-3621-2

[32] Z. Liu, G. Wang, W. Gao, Properties of 310S stainless steel coatings produced by unbalanced magnetron sputter deposition, Materials Characterization, 54 (2005) 466–472. https://doi.org/10.1016/j.matchar.2005.02.001

[33] J. Wang, M. Chen, L. Yang, W. Sun, A. Zhu, F. Wang, Nanocrystalline coatings on superalloys against high temperature oxidation: A review, Corrosion Communications, 2 (2021) 55–62. https://doi.org/10.1016/j.corcom.2021.09.002

[34] R. Kumar, R.K. Singh Raman, S.R. Bakshi, V.S. Raja, S. Parida, Exploring the Influence of Nanocrystalline Structure and Aluminum Content on High-Temperature Oxidation Behavior of Fe-Cr-Al Alloys. Materials, 17 1700 (2024). https://doi.org/10.3390/ma17071700

[35] S. Nasiri, M. Rabiei, A. Palevicius, G. Janusas, A. Vilkauskas, V. Nutalapati, A. Monshi, Modified Scherrer equation to calculate crystal size by XRD with high accuracy, examples Fe_2O_3, TiO_2 and V_2O_5, Nano Trends, 3 (2023) 100015. https://doi.org/ 10.1016/j.nwnano.2023.100015

[36] S. Inoue, T. Saeki, H. Uchida, K. Koterazawa, M. Iwasa, Effect of ion flux on the properties of dc magnetron-sputtered stainless steel films, Vacuum, 66 (2002) 257–261. https://doi.org/10.1016/S0042-207X(02)00151-3

ANALIZA FAZNOG SASTAVA I HRAPAVOSTI NANOKRISTALNIH PREVLAKA NA BAZI ČELIKA 310S SA DODATKOM ALUMINIJUMA

Mariola Spalik [a,*], Barbara Kucharska [b], Aneta Jakubus [a], Grzegorz Krzywoszyja [a]

[a] Univerzitet „Jacob of Paradies", Gorzów Wielkopolski, Poljska
[b] Tehnološki univerzitet u Čenstohovi, Čenstohova, Poljska

Apstrakt

Legiranje aluminijumom se često primenjuje radi poboljšanja otpornosti na visokotemperaturnu oksidaciju. U ovom radu aluminijum je uveden u nanokristalne prevlake dobijene magnetronskim raspršivanjem hrom-nikl čelika 310S. Ispitivan je uticaj dodatka Al na fazni sastav i morfologiju prevlaka, koji imaju značajnu ulogu u formiranju zaštitnih oksidnih slojeva pri visokim temperaturama.

Prevlake su analizirane pomoću skenirajuće elektronske mikroskopije (SEM) i mikroskopije atomskih sila (AFM), sa posebnim osvrtom na hrapavost površine, kao i rendgenske difraktometrije (XRD) radi određivanja veličine kristalita i faznog sastava.

Rezultati su pokazali da dodatak aluminijuma utiče na stabilnost faza u prevlakama. Pri sadržaju Al od 1–2 at.% dolazi do dvostrukog smanjenja udela fcc faze u prevlaci (uz njen potpuni nestanak pri 5 at.% Al), kao i do sličnog smanjenja površinske hrapavosti. Istovremeno, veličina kristalita se povećava uz očuvanje nanokristalne strukture, čime se stvaraju povoljni uslovi za formiranje gustih oksidnih slojeva Al_2O_3 na površini prevlaka.

Ključne reči: *Magnetronsko raspršivanje; Austenitni čelik X8CrNi25-21; PVD prevlake*